Pell-Shear-Exfoliation of few-layer graphene nanoflakes as an electrode in supercapacitors

Exfoliación por cizallamiento de nanohojuelas de grafeno como electrodo en supercondensadores

Author:

ⓘD **Mohammed Aziz Ibrahem[1]**

ABSTRACT

Introduction: The graphene has received a great attention because of its extraordinary characteristics of high carrier mobility, excellent thermal conductivity, high optical transmittance, and superior mechanical strength. Developing a simple methods with the property of producing large quantities of high-quality graphene have become essential for electronics, optoelectronics, composite materials, and energy-storage applications. **Materials and Methods:** In this study, the simple one step and efficient method of grinding was used to produce few-layers graphene nanoflakes from graphite. Different microscopic (TEM, SEM, and AFM) and spectroscopics (XRD, XPS, and Raman) charactrization tools were used to test the quality of the resultant graphene nanoflakes. **Results:** The produced nanoflakes showed no traces of oxidation due to the grinding process. In addition, the applicability of the obtained nanoflakes as potential supercapacitor electrodes was investigated. For that purpose, thin films of the few-layer graphene nanoflakes were developed using spray coating technique. In terms of both transparency and conductivity, the prepared films showed equivalent properties compared to those prepared by more complex methods. The electrochemical properties of the prepared electrodes showed high specific capacitance of 86 F g^{-1} at 10 A g^{-1} with excellent stability. The electrodes sustained their original capacity for more than 7000 cycles and started reducing to 72 F g^{-1} after 10000 cycles. **Conclussions:** The method provides a simple, efficient, versatile, and eco-friendly approach to low-cost mass production of high-quality graphene few-layers. The electrochemical stability and flexibility of the developed thin films indicated that the films could be used as electrodes in a wide range of electronic applications.

[1] Department of Physics, College of Science, University of Duhok, Duhok, Kurdistan Region/Iraq. E-mail: m_aziz7951@uod.ac

INTRODUCCTION

The graphene, an isolated atomic plane of graphite, has received a great attention because of its extraordinary characteristics of high carrier mobility, excellent thermal conductivity, high optical transmittance, and superior mechanical strength. Developing appropriate methods for mass production of high-quality graphene will make it more viable for technological applications. Several preparation methods have been proposed since the rise of graphene such as chemical vapor deposition (CVD) [1-3], wet stirred milling in the presence of different media [4-12]. Intercalation with a wide range of molecules of different materials [17-21], Microwave irradiation of co-intercalated graphite [13]. Laser and plasma irradiation of graphite [14, 15], and reduction of graphite oxide by different solvents [16].

More or less and depending on the targeted application, each of the above mentioned graphene preparation technique has its own merits and limitations. In order to develop a more viable technique feasible for wider range of applications, emphasis must be given to develop a technique which can be cost-effective as well as capable of mass production of high quality graphene with less impurities and defects. To overcome some of the limitations, techniques based on exfoliation of graphite have been the most promising ones so far. Both milling and immersion in different liquid suspensions of graphite have been used for that purpose [17-20].

Because of the high surface to volume ratio of carbon materials causing relatively high specific charge storage, they can be used as an electrode in the energy storage devices such as Supercapacitors. Ideally, a monolayer of sp^2 bonded carbon atoms can reach specific capacitance up to ~550 F/g, large sur-

face area of 2675 m^2/g, high intrinsic mobility of 200,000 $cm^{2/}$(V.s), and optical transmittance around 97.7% [6, 21-25], which basically set the upper limit for all carbon materials. Therefore, an extensive attention is given to utilizing graphene in the supercapacitor device [2, 26-32]. Although supercapacitor electrodes made of graphene powders generally show a high power density, they are limited by the modest capacitance value (~200 $Fg^{-1)}$. Therefore, the energy density and overall device performance are generally unsatisfied. Alternatively, a large capacitance improvement up to 750 F g^{-1} can be achieved by introducing the pseudo-capacitance effects through combining and modifying the carbon electrodes with pseudo-capacitive materials (metals, semi metals, and polymer) [33-35]. On the hand, the capacitance of supercapacitor depends strongly on the electrode materials, and can be optimized by the electrode size and dimension. Among the graphene-based electrodes, graphene thin film have attracted much attention due to the tunable thickness, structural flexibility, lightweight and electrical properties, which are the essential qualities required for supercapacitors. Therefore, tremendous efforts have been dedicated to explore novel processing methods for graphene-based films, such as spray, spin-coating, Langmuir Blodgett, layer-by-layer deposition, interfacial self-assembly, and vacuum filtration. As with other graphene-based materials, the processing of graphene thin films is hindered due to the agglomeration and restacking of graphene sheets resulting from the inter-planar interaction and van der Waals forces, which can greatly reduce the surface areas and limit the diffusion of electrolyte ions between graphene layers [36, 37].

In this study, the two techniques of graphite immersion in liquid suspensions and grinding were combined to synthesis graphene nanoflakes. This meth-

od depends on the effects of pure mechanical forces (shear and fraction). The developed technique offers significant advantages in comparison with other previously mentioned techniques. It is a mild and environmentally friendly (no harsh or toxic reactants) method, it is simple, cheap (based on ball milling) and productive, and potentially can be scaled up to give large quantities (reach litters)) of graphene nanoflakes with high quality, and high stability for long periods of time. More importantly, this very simple technique has the potential for increasing the production tremendously at low cost, offering a promising opportunity to produce graphene in the volumes required for real-world applications. Whereas, these concentrated graphene nanoflakes dispersions could be used to fabricate transparent conductive thin films possess comparable properties to those prepared by more complex methods.

MATERIALS AND METHOD

Nanoflakes preparation: In order to prepare few-layer graphene nanoflakes, the same previous technique for preparing other two dimensional materials has been followed [38, 39]. The pristine graphite powder (Sigma-Aldrich) with particle size > 75 *μm* was used without any further treatment. First, the graphite powder was mixed with pure N-methyl-2-pyrolidinone (NMP, 99 % Macron Chemical, USA) at a concentration of 2 wt%. Next, the prepared graphite suspension was transferred to the grinder (AG-1000, Allgen Technology) which was already half filled with zirconia beads (bead size: 200 mm; density: 5.95 g cm-3). The rotor was set at high rotational speed of 2000 rpm for the duration of 4 hours in order to stir and disperse the prepared dense suspension. Finally, the dark and homogenous suspensions was easily purified from the zirconia beads, the beads

were precipitated at the bottom of the container causing no contamination to the suspension.

Graphene thin film fabrication: In the second part of this work, thin films were fabricated from the previously prepared graphene nanoflakes using simple spray deposition method. First, the graphene nanoflakes were diluted with IPA with 1:1 ratio in order to speed up the draying process. Next, the solution was spray coated onto a substrate which was previously cleaned in ultrasonic bath with acetone and IPA (10 min each step). The spray-coating process was performed in ambient environment (air) inside fume hood. The nozzle diameter and the distance between the sample and the sprayer head were manipulated to obtain a uniform thin film. Finally, the prepared thin films were left in air for 1 h in order to dry off.

Graphene nanoflakes and associated thin films Characterization: Various microscopic and spectroscopic characterization techniques such as TEM (JEM 2100F), SEM (FEI Nova200), XRD (PANalytical), XPS (PHI 5000 Versa Probe scanning ESCA microprobe), AFM (Veeco di Innova), and Raman were used to characterize the prepared few-layer graphene nanoflakes and their associated thin films. The specific surface area measurements were determined using a Digisorb 2006 surface area, pore volume analyzer-Nova Quanta Chrome Corporation instrument using multipoint BET adsorption.

Electrochemical Characterization: In order to characterize the prepared graphene-nanoflakes thin films as supercapacitor electrodes, the cyclic voltammetry (CV) was used. The relative catalytic ability of the prepared films as an electrode was measured. The CV measurements were conducted by using a three-electrode electrochemistry system while the

graphene nanoflakes were used as the working electrode, Pt foil as the counter electrode, and Ag/AgCl as the reference electrode (1 mol/L H_2So_4) for different scanning rate. To determine the capacitance of Supercapacitors, the equation C = 4I $\varDelta t$/mΔV is used to extract the specific gravimetric capacitance [29, 40] where C is the measured capacitance of the two-electrode cell (F/g), I is the constant current (mA), $\varDelta t$ is the discharging time (s), m is the total weight of electrode materials (mg) and ΔV is the voltage drop during discharging process (V). The loaded mass of the active materials was 2.4 mg.

RESULTS AND DISCUSSION

It's believed that there are two scenarios to describe the way graphene nanoflakes were peeled off from the graphite particles using the grinding process. One that the zirconia ball rolls over the top of the surface of the graphite producing a strong shear force (Fig.1a). The second scenario is when the ball first collides with the edge of the graphite particles, producing a high fraction force overcoming the van der Waals interaction, and then slides over its surface (Fig.1b). Additionally, the graphite was mixed with NMP solvent with a surface energy close to graphene's surface energy. This causes a very low energy of mixing [29, 32]. Therefore, it will result in the stabilizing of the exfoliated nanoflakes against aggregation. The sedimentation test showed that the dispersion prepared without grinding precipitated completely within several minutes but the graphene nanoflakes maintained its high quality for a long period of time.
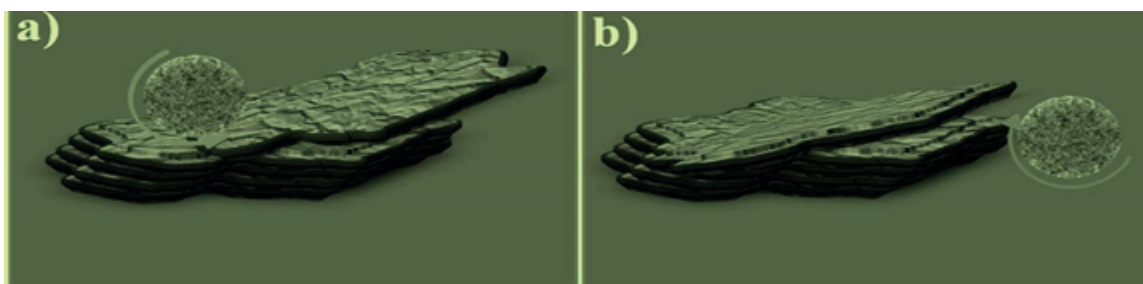
Fig.1 Schematic illustration of the graphene nanoflakes peeling off from the surface of graphite, (a) sliding over the surface scenario and (b) peeling off the edge of graphite particle scenario.

SEM images shown in figure 2a uncovers a large thickness of graphite (>75 μm) and chaotic graphite network. In comparison and as shown in Fig. 2b, the obtained graphene nanoflakes are relatively thin with typical lateral dimensions of few hundred nanometers. Also, the substrate's background can be clearly seen through the nanoflakes confirming the nanoflakes small thickness. Furthermore, AFM technique was used to characterize the topography as well as the thickness of the nanoflakes. Figs. 2b and 2c show a good agreement between both AFM and SEM images in terms the nanoflakes low thicknesses. As shown in Fig. 2d a histogram for height profile of 37 of obtained AFM images, the nanoflakes thickness averaged around four nm. Thus, the average layer number distribution of the graphene nanoflakes is around six layers. The thinnest graphene nanoflakes that have been observed so far acquire an AFM height profile of close to three nm (inset of Fig. 2d).
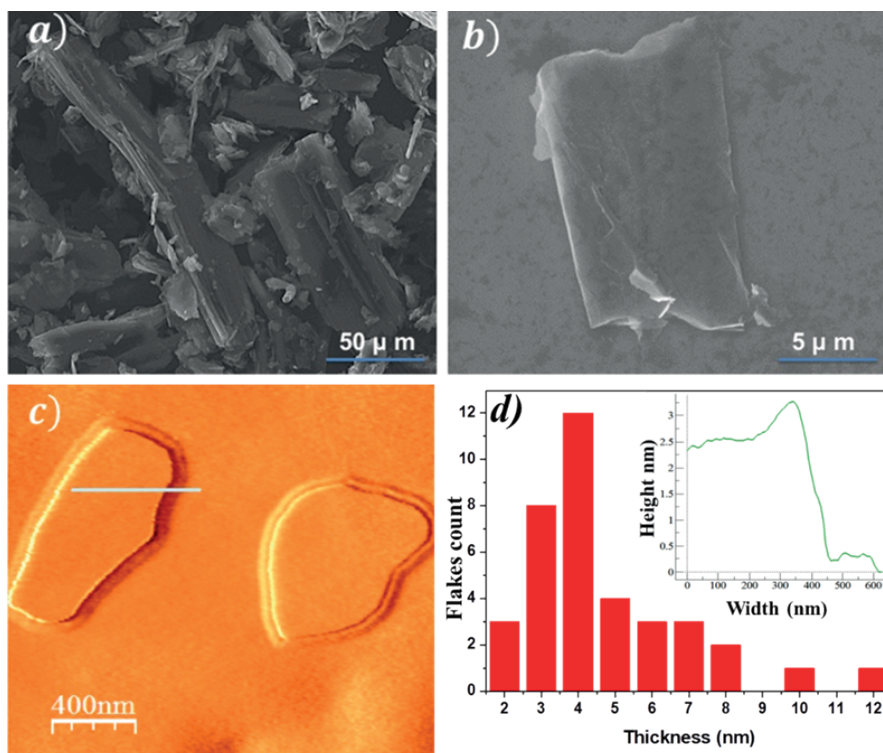
Fig.2 (a, b) SEM images, (c) AFM images, and (d) The histogram of the prepared graphene nanoflakes determined from the AFM images. The inset is a height profiles of corresponding AFM topographies (average thickness: 2.5-3.5 nm) of a typical nanoflake.

TEM imaging and diffraction analysis were used to determine the crystal structure of the obtained graphene nanoflakes. Figures 3a and 3b present TEM images of a typical graphene nanoflake sized several hundred nanometers. The TEM images also show that the obtained graphene nanoflakes thickness is only few nanometers with few layers/ graphene nanoflakes as characterized by SEM and AFM images shown in Fig. 2. The SAED patterns (Fig. 3c and 3e) of the flat areas of nanoflakes and the corresponding high-resolution TEM (HRTEM) images (Fig. 3d and 3f) reveal that the majority of nanoflakes has high crystallinity with hexagonal lattice structure.
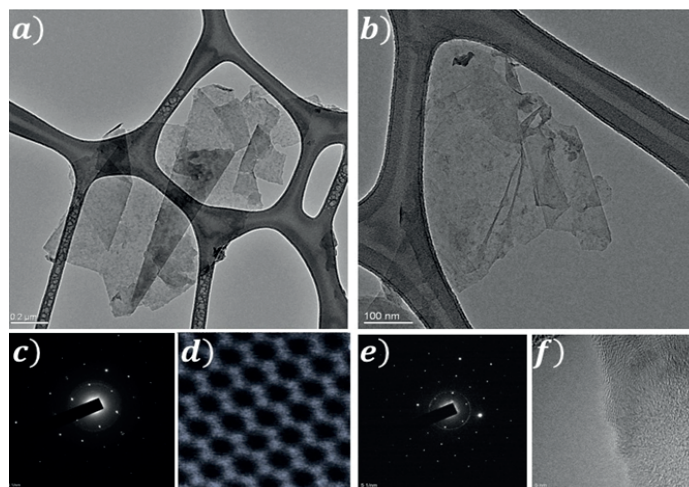
Fig.3 TEM images of graphene nanoflakes (a and b). The selected area electron diffraction (SAED) patterns (c and e) of the flat areas of the nanoflakes and the corresponding high-resolution TEM (HRTEM) images (d and f).

Furthermore, Raman spectroscopy was also used to analyze the crystal quality of the obtained nanoflakes. Figure 4a shows three clear peaks at 1350 cm^{-1} (D-band), corresponds to the breathing mode of sp2 carbon atoms, a very sharp peak at 1580 cm^{-1} (G-band), corresponds to the in-phase vibrations of the graphite lattice, and the 2D-band at 2725 cm^{-1}, an overtone of the D-band [17, 41]. The symmetrical 2D band which can be fitted to one Lorentzian and a 2D/G band ratio of 1.7 is another clear evidence of the fact that the obtained graphene nanoflakes are only few-layers. The spectrum also shows expected two doublets intensity of the 2D bands (D and G) for the majority of the prepared nanoflakes, indicating that the thickness does not exceed few layers. It also confirms that no basal plane defects (no covalently bonded oxides) were introduced during exfoliation [42], which is in agreement with the TEM results. The crystal orientation of the prepared nanoflakes was also characterized using XRD technique. Fig. 4b shows nearly identical diffraction angles for the pristine graphite material and the obtained graphene nanoflakes, however, significant decrease in the intensity and width of nanoflakes peaks were observed. This implies the same degree of crystallinity between graphite and graphene nanoflakes. The corresponding diffraction (peak 2θ at 26.5°) can be assigned to the reflections of the (002) plane, which oriented predominantly along the c-axis or the [002] direction [17, 43]. This is consistent with the HRTEM data shown in Fig. 3. Moreover and in order to quantify the elemental atom ratios and getting further detailed bonding properties of the obtained graphene nanoflakes, XPS analyses were carried out. Fig. 4c shows the expected peaks at 283.9 and 532.1 eV which are attributed to C1s and O1s, respectively. The atomic ratio of C: O of ¼ indicates the existence of small quantity of oxygenated group (Fig. 4d). In addition, the XPS analysis showed a number of smaller features, most probably related to the residual NMP left over from the exfoliation process. [NIST X-ray Photoelectron Spectroscopy (XPS) Database, Version 4.1, http://srdata.nist.gov/xps/][44]]. This can be confirmed simply by determining the ratio of carbon bonding to H, O and N atoms (i.e. C-H, C-N, and C=O). Subsequently, all the spectroscopic analyses showed that the prepared graphene nanoflakes were free of defects and oxides.
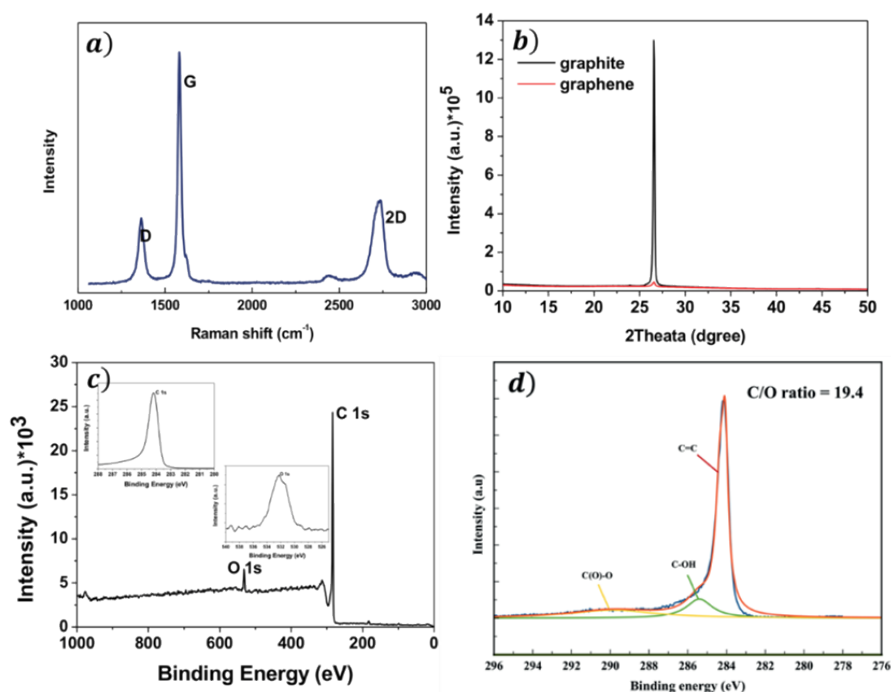
Fig. 4. (a) Raman spectra (Iexcitation. 514 nm) of the prepared graphene nanoflakes (b) XRD patterns of graphite and graphene nanoflakes. (c) XPS survey spectrum and (d) high-resolution XPS C1s spectrum.

Furthermore, the viability of the prepared graphene nanoflakes as a potential technological application was investigated. The prepared graphene nanoflakes solution was spray coated on different substrates of paper, PET, and glass. The obtained semitransparent conductive thin films are shown in Figures 5a, 5b, and 5c, respectively. The resistivity measurements showed that the graphene nanoflakes sample prepared on glass substrate shows resistivity of around 860 Ω, while the thin film on PET substrate exhibited resistivity of around 2 kΩ much lower than 82 kΩ for the sample prepared on paper. The thin films are also flexible and can be shaped into a desired structure without losing their mechanical and electrical

properties. The thin films shows a reasonable stability in terms of their resistivity properties before and after being subjected to various deformations. For example, the thin film prepared on PET had a sheer resistance of 1.98 kΩsq-1 before bending and 2.06 kΩsq-1 after bending. This is another advantage of the prepared films for diversifying their domain of technological applications. The prepared graphene nanoflakes can be used as transparent-conducting films to replace expensive Pt/FTO counter electrodes of dye-sensitized solar cells. Also, it can be used as anode for as anodes of flexible lithium ion batteries and Supercapacitors [45-47].
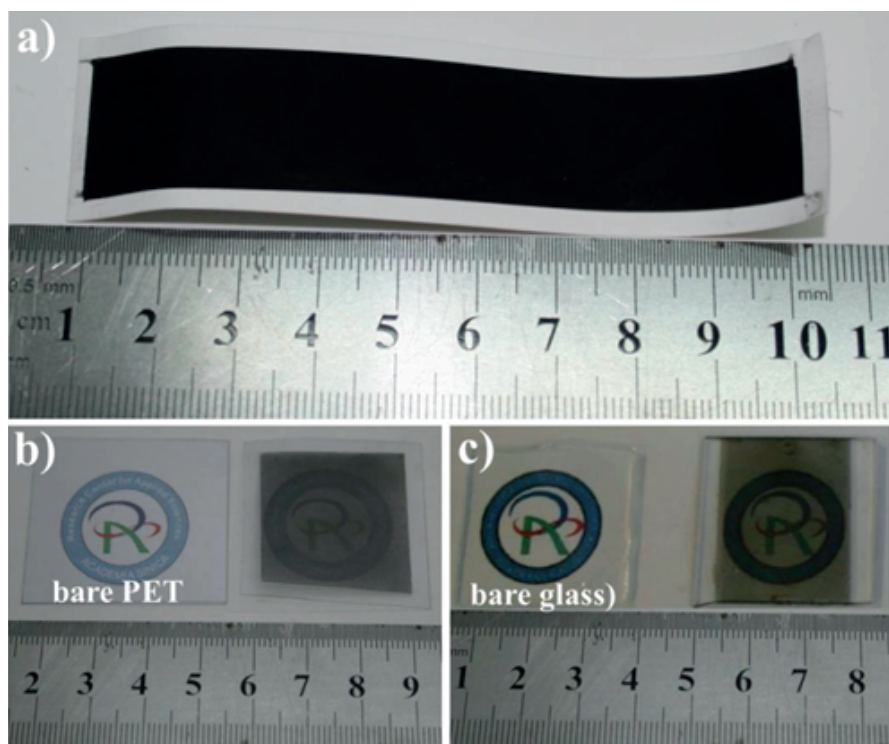
Fig. 5 Large area few layers graphene nanoflakes thin films prepared by spray coating on different substrates (a) paper with length of 10 cm and width 2cm, (b) PET with dimensions 3*3 cm^2, and (c) glass of 4*2.5 cm^2.

Further characterization of the prepared thin films was performed by investigating the electrochemical performance of the film using three-electrode system. Figure 6a shows nearly symmetric rectangular shapes of cyclic voltammetry (CV) curves in 1 mol/L H$_2$So$_4$ at different scan rates even for an

extremely fast scan rate of 100 mV s^{-1} under the current density of 10.0 A g^{-1}. Figure 6b shows a relatively high-rate specific capacitance of 86 F g^{-1} at 10 A g^{-1} and after 7000 cycles the graphene electrode maintained almost its original capacity. However, as expected it start to degrade to retain more than

80% (72 F g^{-1}) after 10000 cycles, revealing an excellent stability for supercapacitor application. This degradation in capacitance can be attributed to the irreversible reaction between the electrodes and electrolyte [48]. Furthermore, as shown in Figure 6b, the charge/ discharge curve of first five cycles observed no obvious change, demonstrating the excellent stability for the graphene nanoflakes as supercapacitors electrode.

For further understanding, the impedance of the graphene nanoflakes electrode before and after the stability test were measured in the frequency range of 100 kHz–0.1 Hz (Fig. 6c). At high frequency region the impedance spectra are almost similar in form of an arc, while it is like a spike at the lower frequency region which is indicating a high electrochemical stability. Furthermore, the equivalent series resistance of the electrode is decreased after 10000 cycles, which can be attributed to the significantly enhanced wettability of the electrode to the electrolyte caused by the relatively loose morphology with highly open pore.[30] In addition, after the long-term cycling, the oblique line of the electrode is more vertical than before, demonstrating that the electrode behaves more closely as an ideal capacitor.
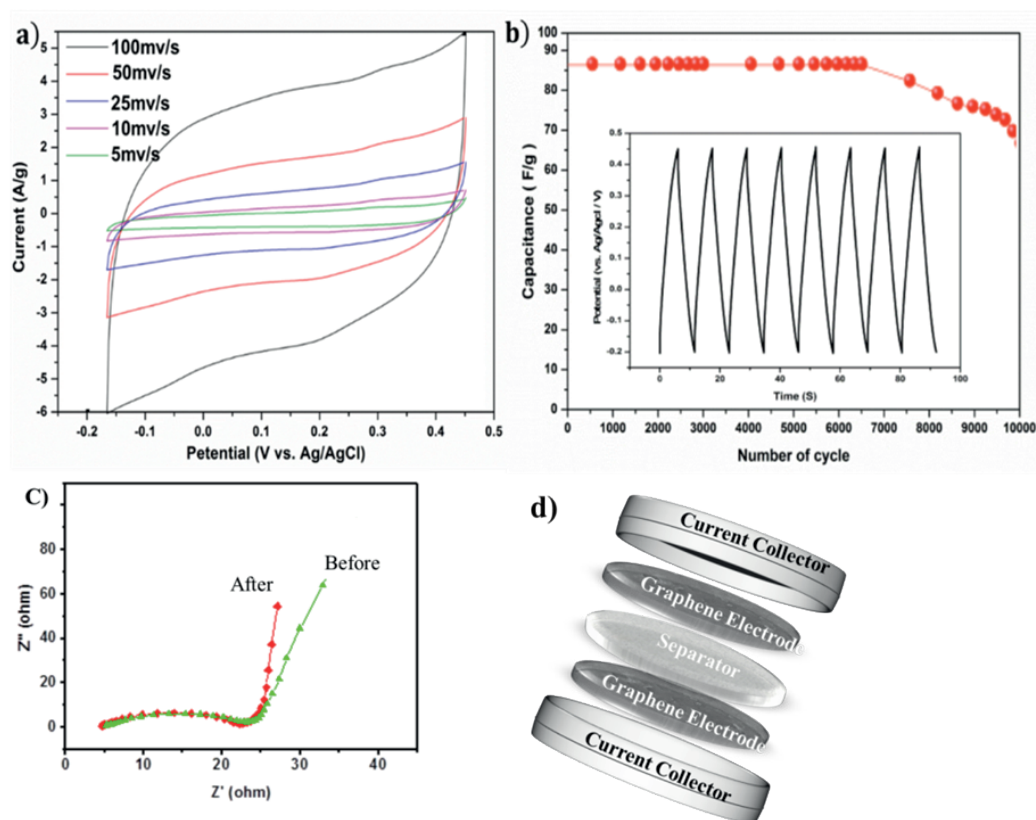
Fig. 6. (a) CV curves with different scan rates. (b)The capacitance retaining and galvanostatic charge/discharge cycles (inset) under constant current density of 10 A g^{-1} in 1 mol/L H$_2$So$_4$ in aqueous solution during 10000 cycles. (c) Nyquist plots for electrode in the frequency range of 100 kHz to 0.1 Hz measured during the cycle life tests. (d) Schematic of the supercapacitor structure.

CONCLUSIONS

The simple method of grinding produced dispersible few-layers of high quality graphene nanoflakes were characterized and investigated. The method provides a simple, efficient, versatile, and eco-friendly approach to low-cost mass production of high-quality graphene few-layers. Integrated with spray coating

technique, uniform semitransparent flexible conductive thin films were developed. The electrochemical stability and flexibility of the developed thin films indicated that the films could be used as electrodes in a wide range of electronic applications.

Acknowledgments

REFERENCES

1. Herron, C., et al. Simple and scalable route for the 'bottom-up' synthesis of few-layer graphene platelets and thin films. Journal of Materials Chemistry, 2011; 21(10): 3378-3383. https://doi.org/10.1039/c0jm03437a
2. Huang, C, et al., Observing the evolution of graphene layers at high current density. Nano Research, 2016; 9(12): 3663-3670. https://doi.org/10.1007/s12274-016-1237-0
3. Sharma, K, et al.. Effect of copper foil annealing process on large graphene domain growth by solid source-based chemical vapor deposition. Journal of Materials Science, 2016; 51(15): 7220-7228. https://doi.org/10.1007/s10853-016-0003-8
4. Shang, N, et al. Controllable selective exfoliation of high-quality graphene nanosheets and nanodots by ionic liquid assisted grinding. Chemical Communications, 2012; 48(13): 1877-1879. https://doi.org/10.1039/c2cc17185f
5. Chabot, V, et al. High yield production and purification of few layer graphene by Gum Arabic assisted physical sonication. 2013; 3: 1378. https://doi.org/10.1038/srep01378
6. Zhao, W, et al. Preparation of graphene by exfoliation of graphite using wet ball milling. Journal of Materials Chemistry, 2010; 20(28): 5817-5819. https://doi.org/10.1039/c0jm01354d
7. Parviz, D, et al. Dispersions of Non-Covalently Functionalized Graphene with Minimal Stabilizer. ACS Nano, 2012; 6(10): 8857-8867. https://doi.org/10.1021/nn302784m
8. Eun-Young, C., et al., Production of graphene by exfoliation of graphite in a volatile organic solvent. Nanotechnology, 2011; 22(36): 365-601. https://doi.org/10.1088/0957-4484/22/36/365601
9. Khan, U, et al. High-Concentration Solvent Exfoliation of Graphene. Small, 2010; 6(7): 864-871. https://doi.org/10.1002/smll.200902066
10. Nuvoli, D, et al. The production of concentrated dispersions of few-layer graphene by the direct exfoliation of graphite in organosilanes. Nanoscale Research Letters, 2012; 7(1): 674. https://doi.org/10.1186/1556-276X-7-674
11. Çelik, Y, Flahaut E., and Suvacı E. A comparative study on few-layer graphene production by exfoliation of different starting materials in a low boiling point solvent. FlatChem, 2017; 1: 74-88. https://doi.org/10.1016/j.flatc.2016.12.002
12. Arao, Y, F. Mori, and Kubouchi M. Efficient solvent systems for improving production of few-layer graphene in liquid phase exfoliation. Carbon, 2017; 118: 18-24. https://doi.org/10.1016/j.carbon.2017.03.002
13. Fu, W, et al. Low-temperature exfoliation of multilayer-graphene material from FeCl3 and CH3NO2 co-intercalated graphite compound. Chemical Communications, 2011; 47(18): 5265-5267. https://doi.org/10.1039/c1cc10508f
14. Lin, C, Lin I, and Tuan W. Effect of graphene concentration on thermal properties of alumina–graphene composites formed using spark plasma sintering. Journal of Materials Science, 2017; 52(3): 1759-1766. https://doi.org/10.1007/s10853-016-0467-6
15. Kumar, P, et al. Growth of few- and multilayer graphene on different substrates using pulsed nanosecond Q-switched Nd:YAG laser. Journal of Materials Science, 2017; 52(20): 12295-12306. https://doi.org/10.1007/s10853-017-1327-8
16. Moon, I, et al. Reduced graphene oxide by chemical graphitization. 2010; 1: 73. https://doi.org/10.1038/ncomms1067
17. Mao, M, et al. Facile and economical mass production of graphene dispersions and flakes. Journal of Materials Chemistry A, 2014; 2(12): 4132-4135. https://doi.org/10.1039/C3TA14632D

18. Chen, X, et al. Direct exfoliation of the anode graphite of used Li-ion batteries into few-layer graphene sheets: a green and high yield route to high-quality graphene preparation. Journal of Materials Chemistry A, 2017; 5(12): 5880-5885. https://doi.org/10.1039/C7TA00459A

19. Río F, et al. A comparative study on different aqueous-phase graphite exfoliation methods for few-layer graphene production and its application in alumina matrix composites. Journal of the European Ceramic Society, 2017; 37(12): 3681-3693. https://doi.org/10.1016/j.jeurceramsoc.2017.04.029

20. Paredes, J, et al. Environmentally friendly approaches toward the mass production of processable graphene from graphite oxide. Journal of Materials Chemistry, 2011; 21(2): 298-306. https://doi.org/10.1039/C0JM01717E

21. Nuvoli, D, et al. High concentration few layer graphene sheets obtained by liquid phase exfoliation of graphite in ionic liquid. J Mater Chem. 2011; 21. https://doi.org/10.1039/C0JM02461A

22. Zheng, S, et al. Graphene-based materials for high-voltage and high-energy asymmetric supercapacitors. Energy Storage Materials, 2017; 6: 70-97. https://doi.org/10.1016/j.ensm.2016.10.003

23. Zhang, K, Yang X, and Li D. Engineering graphene for high-performance supercapacitors: Enabling role of colloidal chemistry. Journal of Energy Chemistry, 2018; 27(1): 1-5. https://doi.org/10.1016/j.jechem.2017.11.027

24. Mendez, J, et al. Charge carrier transport across grain boundaries in graphene. Acta Materialia, 2018; 154: 199-206. https://doi.org/10.1016/j.actamat.2018.05.019

25. Park, J, et al. Direct synthesis of highly conducting graphene nanoribbon thin films from graphene ridges and wrinkles. Acta Materialia, 2016; 107: 96-101. https://doi.org/10.1016/j.actamat.2016.01.029

26. Stoller, M, et al. Graphene-based ultracapacitors. Nano Lett, 2008. 8. https://doi.org/10.1021/nl802558y

27. Zhang, L, Zhou R, and Zhao X, Graphene-based materials as supercapacitor electrodes. Journal of Materials Chemistry, 2010; 20(29): 5983-5992. https://doi.org/10.1039/c000417k

28. Yu, G, et al. Enhancing the Supercapacitor Performance of Graphene/MnO2 Nanostructured Electrodes by Conductive Wrapping. Nano Letters, 2011; 11(10): 4438-4442. https://doi.org/10.1021/nl2026635

29. Liu, C, et al. Graphene-Based Supercapacitor with an Ultrahigh Energy Density. Nano Letters, 2010; 10(12): 4863-4868. https://doi.org/10.1021/nl102661q

30. Yan, J, et al. High-performance supercapacitor electrodes based on highly corrugated graphene sheets. Carbon, 2012; 50(6): 2179-2188. https://doi.org/10.1016/j.carbon.2012.01.028

31. Zheng, S, et al. Arbitrary-Shaped Graphene-Based Planar Sandwich Supercapacitors on One Substrate with Enhanced Flexibility and Integration. ACS Nano, 2017; 11(2): 2171-2179. https://doi.org/10.1021/acsnano.6b08435

32. Wang, S, et al. Scalable Fabrication of Photochemically Reduced Graphene-Based Monolithic Micro-Supercapacitors with Superior Energy and Power Densities. ACS Nano, 2017; 11(4): 4283-4291. https://doi.org/10.1021/acsnano.7b01390

33. Vivekchand, S, et al. Graphene-based electrochemical supercapacitors. Journal of Chemical Sciences, 2008; 120(1): 9-13. https://doi.org/10.1007/s12039-008-0002-7

34. Ke, Q, et al. Surfactant-modified chemically reduced graphene oxide for electrochemical supercapacitors. RSC Advances, 2014; 4(50): 26398-26406. https://doi.org/10.1039/C4RA03826F

35. Papageorgiou, D, Kinloch I, and Young R. Mechanical properties of graphene and graphene-based nanocomposites. Progress in Materials Science, 2017; 90: 75-127. https://doi.org/10.1016/j.pmatsci.2017.07.004

36. Morofuji T, Shimizu A, and Yoshida J. Direct C–N Coupling of Imidazoles with Aromatic and Benzylic Compounds via Electrooxidative C–H Functionalization. Journal of the American Chemical Society, 2014; 136(12): 4496-4499. https://doi.org/10.1021/ja501093m

37. L S, et al. Effect of the Electrolyte Alkaline Ions on the Electrochemical Performance of α-Ni(OH)2/Activated Carbon Composites in the Hybrid Supercapacitor Cell. ChemistrySelect, 2017; 2(23): 6693-6698. https://doi.org/10.1002/slct.201701579

38. Ibrahem, M, et al. Controlled mechanical cleavage of bulk niobium diselenide to nanoscaled sheet, rod, and particle structures for Pt-free dye-sensitized solar cells. Journal of Materials Chemistry A, 2014; 2(29): 11382-11390. https://doi.org/10.1039/C4TA01881H

39. Ibrahem, M, et al. High quantity and quality few-layers transition metal disulfide nanosheets from wet-milling exfoliation. RSC Advances, 2013; 3(32): 13193-13202. https://doi.org/10.1039/c3ra41744a

40. Zhu, Y, et al. Carbon-Based Supercapacitors Produced by Activation of Graphene. Science, 2011; 332(6037): 1537-1541. https://doi.org/10.1126/science.1200770

41. Paton, K, et al. Scalable production of large quantities of defect-free few-layer graphene by shear exfoliation in liquids. Nat Mater, 2014; 13(6): 624-630. https://doi.org/10.1038/nmat3944

42. Li D, et al. Processable aqueous dispersions of graphene nanosheets. Nat Nano, 2008; 3(2): 101-105. https://doi.org/10.1038/nnano.2007.451

43. Johra, F, Lee J, and Jung W. Facile and safe graphene preparation on solution based platform. Journal of Industrial and Engineering Chemistry, 2014; 20(5): 2883-2887. https://doi.org/10.1016/j.jiec.2013.11.022

44. Park S and Ruoff R. Chemical methods for the production of graphenes. Nat Nano, 2009; 4(4): 217-224. https://doi.org/10.1038/nnano.2009.58

45. Xu, C, et al. Graphene-based electrodes for electrochemical energy storage. Energy & Environmental Science, 2013; 6(5): 1388-1414. https://doi.org/10.1039/c3ee23870a

46. Bi, H, et al. Highly conductive, free-standing and flexible graphene papers for energy conversion and storage devices. RSC Advances, 2013; 3(22): 8454-8460. https://doi.org/10.1039/c3ra23500a

47. Pakdel, A, et al. Nonwetting "white graphene" films. Acta Materialia, 2013; 61(4): 1266-1273. https://doi.org/10.1016/j.actamat.2012.11.002

48. Wang Y and Xia Y. Hybrid Aqueous Energy Storage Cells Using Activated Carbon and Lithium-Intercalated Compounds: I. The C/Li Mn 2 O 4 System. Journal of the Electrochemical Society, 2006; 153(2): A450-A454. https://doi.org/10.1149/1.2140678